Lithology and Mineral Resources, Vol. 39, No. 6, 2004, pp. 566–579. Translated from Litologiya i Poleznye Iskopaemye, No. 6, 2004, pp. 651–666.

History of Holocene Sedimentation in the Southern Kara Sea

M. A. Levitan[1], M. V. Bourtman[2], L. L. Demina[2], V. V. Krupskaya[1], E. M. Sedykh[1], and M. Yu. Chudetsky[3]

[1] *Vernadsky Institute of Geochemistry and Analytical Chemistry, Russian Academy of Sciences, ul. Kosygina 19, Moscow, 119991 Russia*
e-mail: levitan@geokhi.ru
[2] *Shirshov Institute of Oceanology, Russian Academy of Sciences, Nakhimovskii pr. 36, Moscow, 117218 Russia*
e-mail: murdma@sio.rssi.ru
[3] *Institute of Oil and Gas Problems, Russian Academy of Sciences, ul. Gubkina 3, Moscow, 119991 Russia*
e-mail: chudetsky@mail.ru

Received October 17, 2003

Abstract—Two bottom sediment cores (BP00-23/7 and BP00-7/6) recovered from the Yenisei transect in the southern Kara Sea are described. Data on their grain size composition, clay and heavy mineral assemblages, and distribution of a large group of chemical elements are presented. Radiocarbon dates based on AMS C-14 method suggest the Holocene age of sediments in the cores. Literature data on physical properties and foraminifers have also been analyzed. The facies affiliation of the lithostratigraphic subdivisions has been unraveled. History of the Yenisei River runoff in the Holocene has been reconstructed on the basis of different indicators.

INTRODUCTION

River runoff in the Arctic Ocean has a strong impact on the sea ice formation, water column stratification, thermohaline circulation, and other parameters related to the Arctic climate. The Yenisei River accounts for nearly one-fourth of the annual river runoff into this ocean (Aagaard and Carmack, 1989). Therefore, the Yenisei runoff history is very important for understanding the Arctic paleoclimate.

The study of the early Pleistocene–Holocene history of the Kara Sea was restrained for a long time owing to the absence of a reliable geochronological database. Researchers were compelled to use lithostratigraphic and (Kosheleva and Yashin, 1999) or ecostratigraphic (Levitan *et al.*, 1994) models. Publications devoted to this issue based on radiocarbon dates obtained by the AMS C-14 method began to appear only since the second half of the 1990s (Levitan *et al.*, 2000; Hald *et al.*, 1999; Polyak *et al.*, 1997, 2000, 2002; Stein *et al.*, 2002). These publications marked, in particular, that the early Holocene sedimentation rate was higher in the major part of the Kara Sea owing to powerful discharges of the Ob and Yenisei rivers and the sedimentation rate subsequently decreased.

The chemical and mineral compositions of bottom sediments of the Kara Sea have been described in several publications (Belov and Lapina, 1961; Gurvich *et al.*, 1994; Gurevich, 1995; Schoster and Stein, 1999; Siegel *et al.*, 2001a, 2001b; Levitan *et al.*, 1996, 2002). However, works devoted to the evolution of the chemical and mineral compositions of bottom sediments of the Kara Sea based on a reliable geochronological database and linked to the Holocene sedimentation history are still absent. The present communication provides the first insights into the issue formulated above. Particular attention is given to the Yenisei runoff history based on the lithological, mineralogical, and geochemical data. Micropaleontological indicators are also discussed on the basis of literature data.

MATERIALS AND METHODS

We studied bottom sediments from cores BP00-23/7 (73°28.5′ N, 79°51.3′ E; water depth 33 m) and BP00-7/6 (74°39.5′ N, 81°08.5 E; water depth 38 m) recovered from the Yenisei transect during the R/V *Akademik Boris Petrov* cruise under the framework of the joint Russian-German SIRRO project in 2000. Results of the macroscopic description and comprehensive investigation of smear-slides (Stein and Levitan, 2001) were supplemented with data on the water content and bulk density of natural sediment obtained by the weight analysis (Kodina *et al.*, 2001). The grain size analysis was performed by the combined method (Petelin, 1967) in the Analytical Laboratory of the Shirshov Institute of Oceanology under the supervision of V.P. Kazakova. In order to achieve good correlation with the respective data obtained by our German colleagues, grain sizes of 0.05 and 0.002 mm were accepted as the sand–silt (aleurite) and silt–clay (pelite) fraction boundaries,

0024-4902/04/3906-0566 © 2004 MAIK "Nauka/Interperiodica"

Table 1. Radiocarbon age of the bivalve *Portlandia* shell samples

Lab. no.	Core	Unit, cm	Weight, mg	$\Delta^{13}C$	^{14}C age, yr
AA44370	BP00-07/6	240	77	–2.76	4185 +/– 43
AA44371	BP00-07/6	645	108	–2.86	7482 +/– 50
AA44372	BP00-23/7	137	79	–4.04	8607 +/– 50
AA44373	BP00-23/7	290	36	–5.00	8891 +/– 62

respectively. Names of lithotypes of sediments in the Russian version of this communication are given according to (Frolov, 1995).

The mass-spectrometric radiocarbon analysis in the Arizona University accelerator facility was financially supported by the grant of the Bird Polar Research Center. Results of the examination of bivalve mollusk (*Portlandia arctica*) shells are given in Table 1. In order to carry out the subsequent calculations, the obtained dates were corrected for the reservoir age of 440 yr (Stein *et al.*, 2002) and transformed into the calendar age in accordance with the method described in (Stuiver *et al.*, 1998). All dates in the present communication are given in the calendar age scale (cal BP00).

The chemical composition of sediments was analyzed at the Vernadsky Institute of Geochemistry and Analytical Chemistry by the INAA method described in (Kolesov, 1994). In addition, concentrations of several elements were determined by the ICP-AS and atomic absorption methods (Sedykh *et al.*, 2000). Characteristics of the studied sediments are supplemented with results of the semiquantitative determination of benthic foraminifer population (Ivanova, 2001) and the analysis of clay and heavy mineral assemblages carried out by V.V. Krupskaya and M.V. Bourtman, respectively. The clay minerals were analyzed in the <0.001 mm fraction, while the heavy minerals were examined in the heavy subfraction (separated by bromoform with n = 2.89 g/cm^3) of the 0.1–0.05 mm fraction.

RESULTS AND DISCUSSION

Core BP00-23/7

In the Gulf of Yenisei, one can recognize the following subfacies zones of recent sediments (from south to north): subaerial delta, submarine delta, proximal marginal-filter zone, depocenter, and distal marginal-filter zone (Fig. 1). Core BP00-23/7 is located in the distal zone.

Lithological and grain size fractions. Sediments of Core BP00-23/7 include the following lithostratigraphic units (from top to bottom):

(1) 0–85 cm. Olive-gray to dark olive-gray and black sandy–silty clay with a coarse sandy–silty clay (hereafter, coarse silt) interlayer in the middle part. Two wood fragments (1–3 cm) were detected at 0–25 cm and a bivalve mollusk fragment was found at 24 cm. At 25 cm and downsection, one can see black spots of hydrotroilite and bioturbation of low and medium intensities. The studied sediment has the following average composition, %: clay minerals 50, quartz 25–30, and feldspars 10–15. Rock fragments and heavy minerals account for as much as 5–7% of the sediment at the upper (0–25 cm) interval and does not exceed 3–5% at the lower interval. Diatoms and plant remains account for less than 5%. The benthic foraminifer population is rare (2–5%).

The sand fraction (Fig. 2) varies form 13 to 20% at the upper (0–60 cm) interval and abruptly drops to 8% at the lower interval. In contrast, the silt content increases from 27–30% at the upper interval to 34% at the base. The clay content remains stable at 52–57%. The water content drastically decreases from 52 to 40% at the upper (0–25 cm) interval and increases to 50% at the lower interval. The bulk density gradually increases downsection from 1.20 to 1.40 g/cm^3.

Thus, unit 1 can be subdivided into the upper (0–25 cm) and lower (25–85 cm) subunits.

(2) 85–335 cm. Olive-gray silty clay. Black sediment layers, 2–4 thick, are developed at 144–159 and 183–192 intervals. Bivalve mollusk detritus is found at 88, 120, 137, and 290 cm. Unit 2 is characterized by the abundance of hydrotroilite patches and coatings and moderate or strong bioturbation. Relative to the upper unit, Unit 2 is depleted in quartz and enriched in clay minerals and plant remains. The benthic foraminifer population remains rare at 90–230 cm and increases to the normal content (5–10%) at the lower interval.

One can recognize two intervals (85–175 and 175–335 cm) in terms of the grain size composition. The first interval is characterized by the downcore decrease of the sand and silt contents (8–1 and 36–28%, respectively) and increase of the clay content (57–72%). In the lower interval, the sand content varies from 0.7 to 2.1%, the total silt content increases from 30 to 38%, and the clay content decreases from 70–72% to 61%. Beginning from 230 cm, the decrease of the clay content becomes more prominent, probably, owing to the increase of foraminifer remains. In the upper interval, the water content is virtually stable (50–52%); the bulk density decreases from 1.40 to 1.20 g/cm^3 at 130 cm, increases to 1.47 g/cm^3 at 130–140 cm, and remains stable downward the section. In the lower interval, the water content remains 50–52% up to the level of 230 cm. Downward this level, the water content at first drastically decreases to 42% and

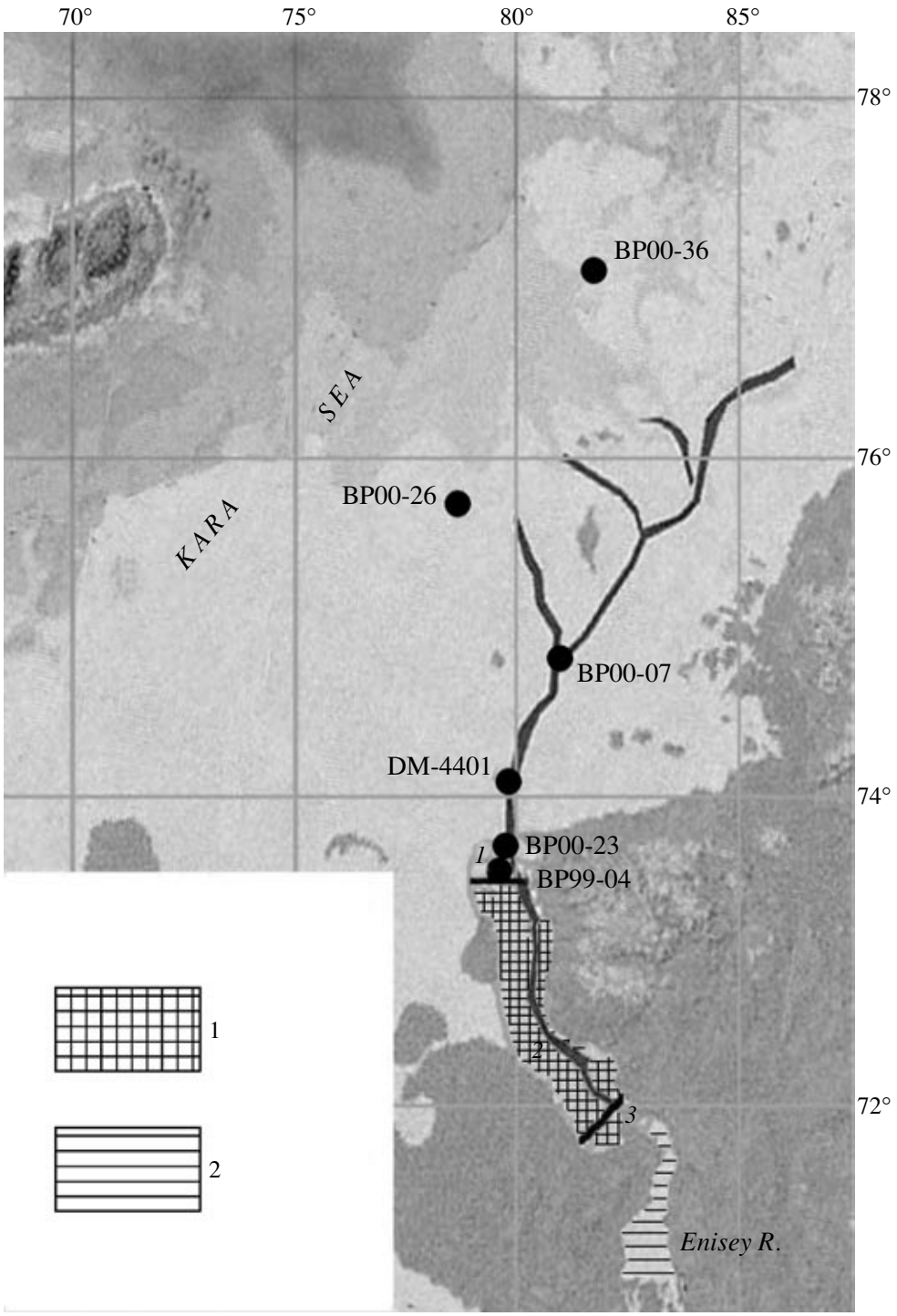

Fig. 1. Location of geological stations along the Yenisei transect of the Kara Sea. (1) Marginal filter: (*1*) distal zone, (*2*) depocenter, (*3*) proximal zone; (2) delta.

then rises to 50%. The bulk density is 1.47 g/cm^3 and increases to 1.50 g/cm^3 at 280 cm. Thus, the available data make it possible to divide Unit 2 into three subunits (85–175, 175–230, and 230–335 cm).

(3) Unit 3. Olive-gray slightly bioturbated sandy–silty clay and coarse silt with an appreciably lower content of clay minerals. The concentration of fragments of rocks and heavy minerals (including black ore minerals) is dramatically increased. Benthic foraminifers are rare.

The grain size composition is as follows (%): sand fraction 14–16, silt fraction 33–38, and clay fraction 50. The water content decreases downsection from 50 to 24%. The bulk density is 1.47 g/cm^3.

(4) 374–427 cm. Olive-gray clayey–sandy silt and clayey–silty sand (at the base) with a distinct horizontal-bedded structure of interlayers 1–2 cm thick. The clay mineral content is very low (up to 5–10%) at the core base. The rock detritus content increases to 25%. The concentration of heavy minerals, primarily, black ore minerals is drastically increased. The sediments contain abundant plant remains and fresh-water diatom frustules. Benthic foraminifers are absent.

The sand content is 32% in silty interlayers and 44–47% in sandy interlayers. The silt content is 50 and 24–27%, respectively. The clay content is as much as 26–31%. The water content and bulk density are up to 30% and 1.75 g/cm^3, respectively, at the core base.

Mineral composition. As is evident from Fig. 2, the clay mineral assemblage is rather monotonous in the <0.001 mm fraction, %: smectite 34.2–44.3% (average 38.3%), illite 35.6–41.8 (average 39.5), kaolinite 6.8–13.5 (average 9.9), and chlorite 8.1–15.7 (average 12.3%). The average smectite/illite ratio is 1.0 (0.9 in the majority of cases), while the chlorite/kaolinite ratio is 1.2. The smectite/illite ratio slightly increases at the core base and in the surface layer. The chlorite–smectite–illite assemblage prevails in the sediments.

In contrast, the heavy mineral fraction (0.1–0.05 mm) demonstrates a distinct trend (Fig. 2): the clinopyroxene/epidote ratio and the average clinopyroxene content decrease downward the section. The downcore decrease of the content of black ore minerals is not so distinct. Like the smectite/illite ratio, the clinopyroxene/epidote ratio increases in the surface layer and the lower half of the core. The content of iron hydroxides and grains with a ferruginous coating rises in the middle section of Unit 2. The surface layer is significantly enriched in basaltic hornblende, enstatite-hypersthene, titanite, fluorite, andalusite, muscovite, sillimanite, and rock fragments.

Chemical composition. One can subdivide the distribution of chemical elements and their ratios in the studied sediments into the following five conditional (sand, silt, clay, feldspar, and epidote) types. In the sand type, the La/Yb ratio rises in the upper and lower intervals relative to the middle interval (Fig. 3). This can naturally be explained by the geochemical behavior of LREE and HREE and the grain size composition of sediments. The silt type is marked by a more or less stable concentration of Zr, Cd, Ni, and Ti, as well as Ce/La, Eu/Sm, and La/Sm ratios (Fig. 3). Some of these elements are concentrated in the silt. The silt content is less variable than the sand or clay content.

The clay-type distribution (concentration in the middle interval and decrease in the upper and lower intervals) is inherent to Al, Fe, Mn, P, U, Mo, Cu, Zn, Co, Cr, Th, Sc, Yb, and Lu (Fig. 3). The Al and Fe distribution deserves a special attention. Evidently, Al is mainly concentrated in the crystal lattice of clay minerals. The Fe content increases from 2.0–2.5% in sediments of Unit 4 to 6.0–6.5% in the middle interval of Unit 2. The latter interval is characterized by rather high contents of iron hydroxides and grains with the ferruginous coating (~20%). Since the Al concentration is maximal in the entire Unit 2, the Fe concentration lag (relative to Al) should be attributed to the phenomenon observed in the present-day mixing zones of river and sea waters—the shift of maximal Fe concentrations toward the depocenter where Fe is extensively transferred from the true dissolved state to the colloidal state and precipitated as colloidal particles and organic iron compounds. Such processes take place in the present-day surface water of the Gulf of Yenisei at a salinity of 5‰ (Dai and Martin, 1995). In contrast, Al concentrated in clay minerals already start to precipitate in the proximal marginal-filter zone at the beginning of the mixing of river and sea waters. This process continues up to the frontal-filter zone. The major part of minor elements of the studied assemblage is associated with clay minerals or unaltered iron compounds. Therefore, the behavior of minerals can also explain the behavior of minor elements. In this connection, it is worth mentioning that the Sc behavior exactly mimics the Fe distribution (Fig. 3). A certain role is played by the coagulation of dissolved organic matter simultaneously with the transformation of iron forms (Artem'ev, 1993).

The feldspar-type distribution includes only Sr that steadily increases downward the section (Fig. 3). This phenomenon can probably be explained by the predominance of fluvial fragments at the core base. In (Levitan *et al.*, 1998), we demonstrated that the majority of feldspars (first of all, calcic and intermediate plagioclases) are derived from the Yenisei River runoff. The carbonate content does not exceed a few percents in the studied sediments. Hence, the major portion of Sr is concentrated in crystal lattices of feldspars (particularly, potassic varieties) that prevail in the sediments (Levitan *et al.*, 1998).

Finally, the epidote-type distribution is typical of Hf, Pb, Cs; La, Ce, Nd, Sm, and Eu. Their concentrations decrease downward the section (Fig. 3). This can be explained by changes in the sedimentation environment from the submarine delta (Unit 4) to the proximal marginal-filter zone (Unit 3), depocenter (Unit 2), and distal marginal-filter zone with the participation of products of the coastal abrasion of the Taimyr Peninsula (Unit 1). Indeed, such behavior of REE during the transition from the alluvial facies to the coastal-marine facies has long been described in (Balashov, 1976). Based on the study of REE behavior, we revealed that the basal sediments (370–400 cm) are close to the Siberian trap basalt, while sediments of Unit 1 are similar to platform sedimentary rocks (Table 2).

Sedimentation and sedimentary mass accumulation rates. Based on the radiocarbon dates (cal BP00) coupled with their linear interpolation and extrapolation, the age and sedimentation rate of Unit 2 are esti-

Table 2. REE contents (ppm) in sediments of the Yenisei marginal filter

Elements	Bottom sediments in Core BP00-23/7		Trap basalts of the Putoran Plateau, Mokulaev Formation (Lightfoot *et al.*, 1990)	Platform sedimentary rocks (Balashov, 1976)
	Interval 0–80 cm (n = 7)	Interval 370–400 cm (n = 6)		
La	30.0	17.3	6.9	35.5
Ce	56.1	32.0	16.5	67.0
Nd	23.2	13.2	11.2	33.0
Sm	6.53	3.3	3.21	6.7
Eu	1.19	0.47	1.11	1.24
Tb	0.95	0.62	0.65	1.0
Yb	2.28	2.86	2.36	2.95
Lu	0.37	0.25	0.36	0.45

mated at 9.2–9.6 ka and 475 cm/ka, respectively. In this case, the sedimentation rate of Unit 1 is 10.5 cm/ka. Taking into consideration the grain size composition in sediments of Unit 1, one can affirm that the sedimentation rate is decreased to a certain extent upward the section. Assuming the radiocarbon age boundary of units 3 and 4 at 10 ka (Polyak *et al.*, 2000, 2002; Stein, 2001), the sedimentation rate in Unit 3 of the age scale accepted in our work is equal to ~20 cm/ka. The sedimentation rate is unknown for Unit 4. Taking into consideration the data on water content and bulk density of the natural sediments, the sedimentary mass accumulation rate (hereafter, mass accumulation rate) is ~8.2 g/cm^2/ka for Unit 1, 357.5 g/cm^2/ka for Unit 2, and 20.6 g/cm^2/ka for Unit 3.

Sedimentation history. The analysis of the material discussed above suggests that the basal section of Core BP00-23/7 includes the submarine delta-facies sediments accumulated in a fresh-water zone of the Yenisei River 11.3 ka BP00 (Unit 4). This interpretation is also supported by the absence of benthic foraminifers in these sediments. In the present-day sediments of the studied region, the benthic foraminifers disappear precisely in the submarine delta-facies sediments where the bottom water salinity equals to zero (Khusid and Korsun, 1996). Judging from the mineral and chemical composition, the relatively coarse-grained fraction of sediments of Unit 4 is primarily composed of erosion products of the Putoran Plateau basalt and its weathering crust.

Unit 3 includes the relatively fine-grained sediments of the proximal marginal-filter zone (Levitan, 2001). The zero isohaline line existed in surface water of this area 11.3 ka BP00. Subsequently, the salinity gradually increased to ~4‰ up to 9.6 ka BP00. Hydrodynamic barrier in the collision zone of active currents of the submarine delta with the calm seawater mass mediated the preferential precipitation of the relatively coarse-grained fraction, the sedimentary mass accumulation rate being equal to ~20.6 g/cm^2/ka.

The depocenter formed in a few hundred years in the studied Gulf of Yenisei area. A large volume of clayey material contained in the water suspension of the mixing zone settled on the bottom. When the salinity of the surface water reached 5‰ approximately 9.4 ka BP00, this material was supplemented with a large amount of Fe, organic matter, and minor elements. The sedimentation rate reached very high values (357.5 g/cm^2/ka). Sediments of Unit 2 formed according to this scenario. Such dramatic events could only be provoked by the vigorous and rapid rise of water content in the Yenisei River drainage area as a result, for example, of the warming (MacDonald *et al.*, 2000) and the consequent active degradation of the permafrost. Numerous examples of high sedimentation rates in the considered time interval have been cited for the Kara Sea in (Polyak *et al.*, 1997, 2000, 2002; Stein *et al.*, 2002).

After 9.2 ka BP00, the sedimentation rate drastically decreased mainly due to the reduction of clay fractions. At the same time, the sediments were passively enriched in coarser fractions. Since the role of river runoff relatively diminished, the silty–sandy material delivery was mainly related to products of the coastal abrasion of the adjacent Taimyr Peninsula that was composed of Lower Paleozoic clastic–clayey sediments of the greenstone facies (*Geologicheskoe…*, 1984). Based on mineralogical data, one can assume the relative increase of the contribution of river runoffs only for the uppermost layers of Unit 1, the precise age of which is unknown. The mass accumulation rate was 8.2 g/cm^2/ka, on the average, and the salinity of surface water in the studied area increased from ~10 to 20‰.

Distal sediments have an insignificant thickness in Core BP00-23/7. Therefore, we cannot describe in detail the history of river discharges in the latest 9.2 ka for this area. However, results of the study of sediments in the adjacent Core BP0099-04/7 (Fig. 1) provide such an opportunity (Stein *et al.*, 2000, 2002; Polyakova and Stein, 2002).

In this core, the boundary between the proximal marginal-filter zone and depocenter passes at 9.25 ka

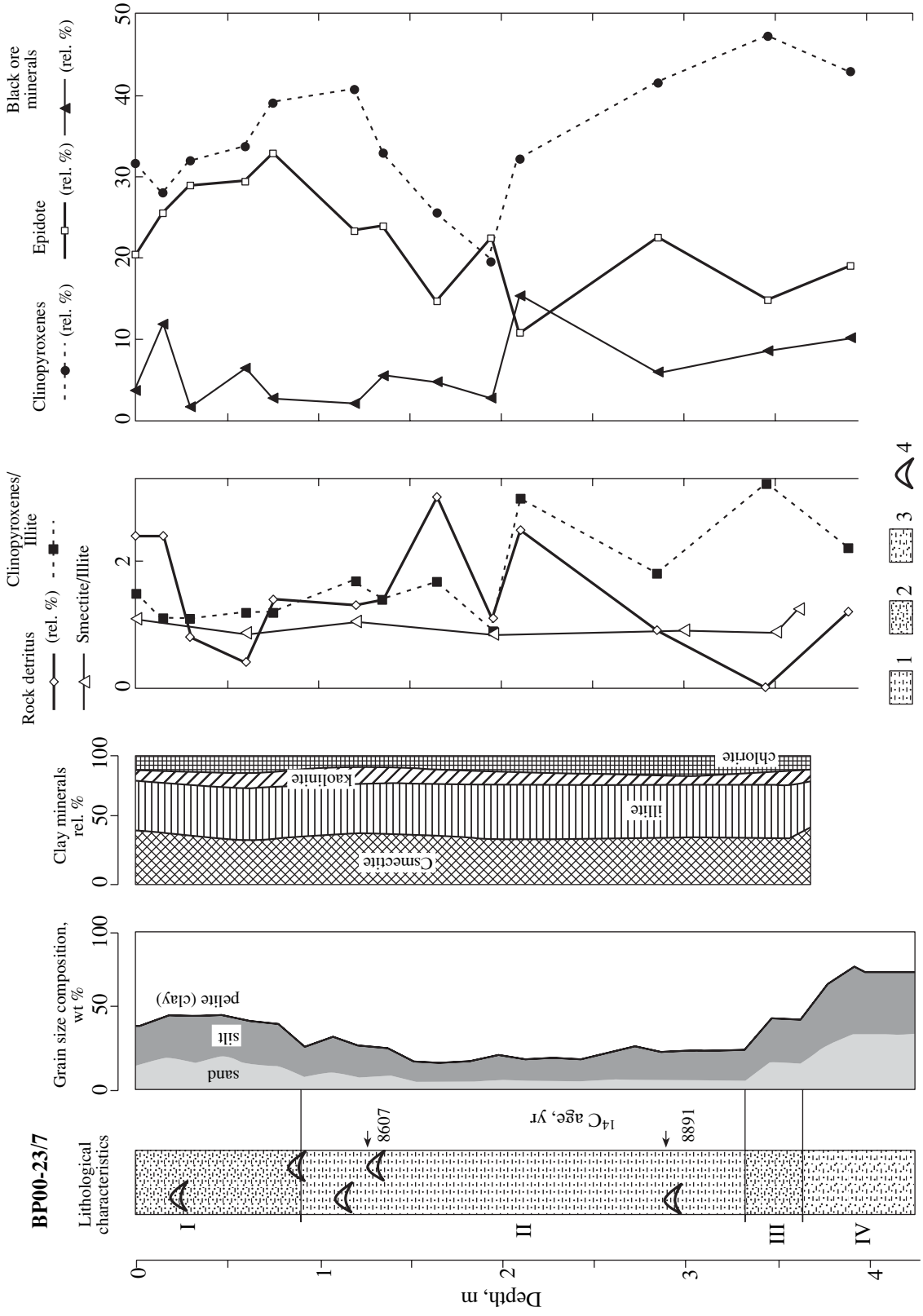

Fig. 2. Mineral composition of sediments in Core BP00-23/7 and distribution of some minerals in them. (I–IV) Lithostratigraphic units. Arrows show the radiocarbon dates (see Table 1). (1) Silty clay; (2) sandy–silty clay; (3) clayey–sandy silt and silty sandy; (4) bivalve mollusk shells.

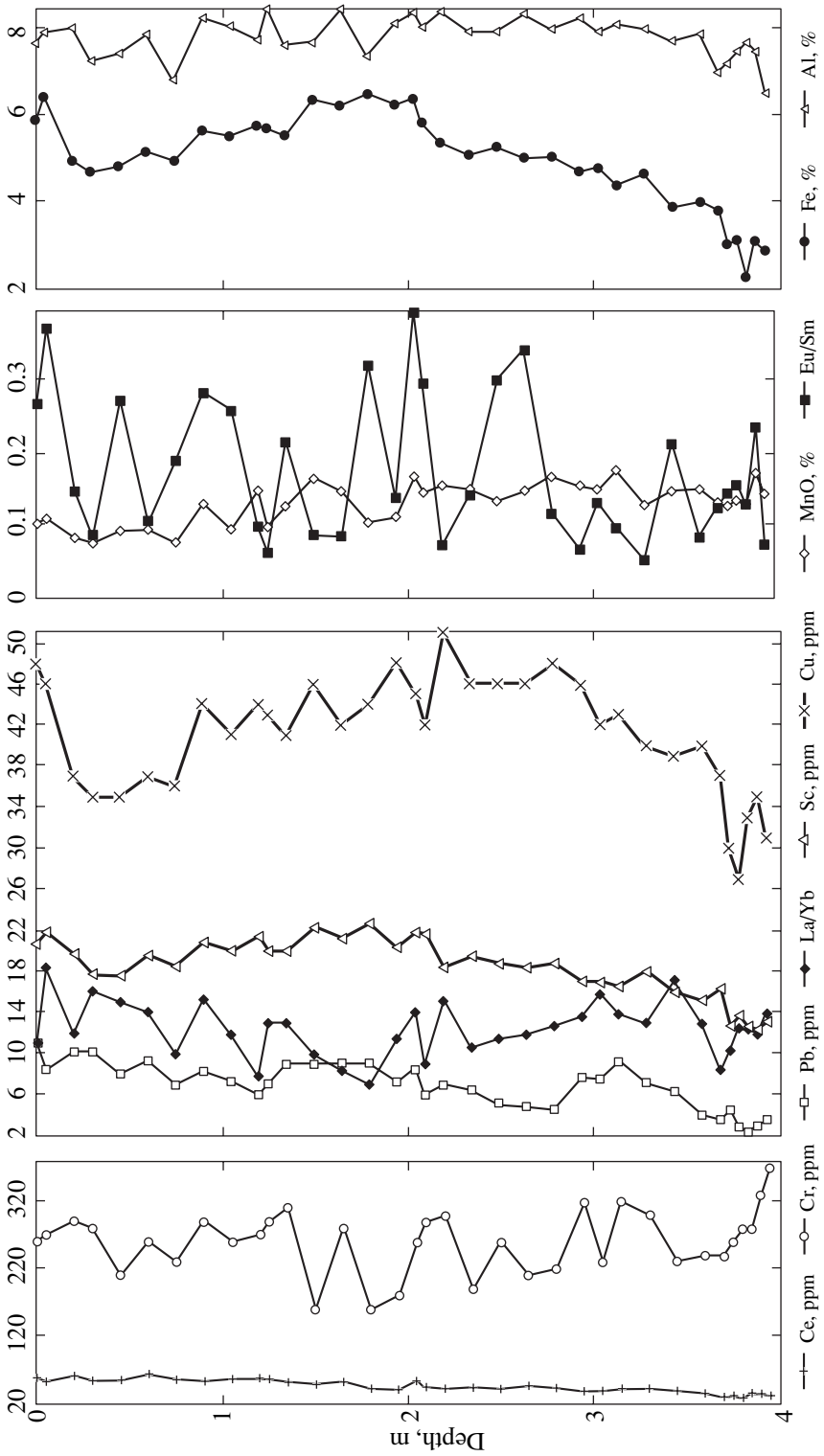

Fig. 3. Vertical distribution of some chemical elements and their ratios in Core BP00-23/7.

BP00. The significant attenuation of magnetic susceptibility, probably, related to the decrease of the concentration of ferromagnetic substances delivered during the erosion of Putoran traps, is recorded at the level of 650 cm (Stein *et al.*, 2000) or 8.74 ka BP00. The significant (two times) decrease of sedimentation rate took place after 8.0 ka BP00.

Core BP00-7/6

Core BP00-7/6 is located slightly north of Core BP00-23/7 in a sediment-filled channel, one of the river valleys of the hydrographic network of the ancient Yenisei River on the Kara Sea shelf (Fig. 1).

Lithology and grain size composition. The studied core can be subdivided into the following lithostratigraphic units (from top to bottom):

(1) 0–510 cm. Silty clay with single pelitic sediment interlayers (Fig. 4). Dark olive-gray and dark gray sediments prevail in the 0–365 cm interval. Dark gray and black sediments predominate in the lower interval. Sediments of the 0–25 cm interval have a homogeneous structure. They are moderately or strongly bioturbated in the lower interval. Hydrotroilite patches and coatings are universally developed in the section. Bivalve mollusk shells are found at 237 and 270 cm. The sediments are composed of clay minerals (50–75%), quartz (25–50%), and feldspars (5–10%). The content of heavy minerals and rock fragments does not exceed 5%. Locally, the rock detritus content increases to 8–10% (e.g., at 49 m) and plant remains are found (e.g., at 325 and 430 cm). The benthic foraminifer content is generally in the range of 5–10% and decreases to 2–5% below the level of 430 cm.

The average grain size composition is rather monotonous and stable, %: sand fraction 2, silt fraction 30, clay fraction 68 (Fig. 4). The water content decreases from 70% at the surface to 50% at the Unit 1 base. Intermediate maximums are recorded at 100, 200, and 350 cm. A prominent minimum is observed at 150 cm. The bulk density inversely correlates with the water content and increases from 1.15 g/cm^3 at the surface to 1.35 g/cm^3 at the base. Bulk density fluctuations are similar to those of the water content.

(2) 510–665 cm. Dark gray and black silty–sandy clay with rare pelitic sediment interlayers and single sandy–silty clay strata (525 and 568 m). The sediments are moderately or strongly bioturbated. Bivalve shells are found at 544 and 644 cm. The sediments are compositionally similar to those in Unit. However, the coarser-grained interlayers are depleted in clay minerals and enriched in rock and heavy mineral fragments. Plant remains are absent. The benthic foraminifer content is generally 2–5% and increases to 5–10% only below the level of 610 cm.

The grain size composition is characterized by a strong variability typical of layered sediments. The composition of thin silt layers is approximately similar to that in Unit 1. The coarser-grained variety is enriched in sand (up to 17%) and silt (up to 39%) and depleted in clay (51%). It is worth noting that both sand and silt fractions display an independent distribution mode in the core. The water content decreases to 45% downward the section with some fluctuations. The bulk density virtually remains at the previous level and weakly responds to changes in the grain size composition.

Mineral composition. The clay minerals are mainly represented by the kaolinite–chlorite–smectite–illite assemblage (Fig. 4). The composition is as follows, %: smectite 21.6–45.2 (average 30.5), illite 28.5–50.4 (average (42.8)), kaolinite 8.0–14.9 (average 10.9), and chlorite (12.9–21.2) (average (15–8)). The average smectite/illite and chlorite/kaolinite ratios are 0.7 and 1.5, respectively. The smectite/illite ratio appreciably increases at 195 and 600 cm (more than 1.0). This value is equal to 0.9 in Unit 1 (45–110 and 405 cm). The minimal value (0.4) is typical of the lower unit. In general, the smectite/illite ratio is slightly higher in Unit 1 relative to Unit 2.

The heavy mineral composition shows a distinct trend of upsection increase of the pyroxene/epidote ratio (Fig. 4). This ratio is more than 0.8 at 650, 590, 500–520, 320, 145–210, 60, and 0–20 cm. In general, intervals of the high pyroxene/epidote ratio virtually coincide with those of the high smectite/illite ratio noted above. Concentrations of clinopyroxene, hydrotroilite, black ore minerals, titanite, and chlorite show a less distinct growth trend in the same direction. The epidote content decreases upward the section. Sediments of Unit 2 are commonly enriched in aegirine-augite and rock detritus relative to Unit 1, which is slightly enriched in tourmaline, Cr-spinel, and volcanic glass. Other minerals are uniformly distributed.

Chemical composition. The chemical composition of the sediments is characterized by a very low variability along the core. In any case, we can confidently affirm the existence of a single provenance and accumulation of chemical elements in similar constraints. We have recognized two groups of elements that mainly differ in terms of the type of material that absorbed the elements from seawater. Elements of the first group (Sc, Co, Cr, Sb; La, Ce, Nd, and Sm) were absorbed by iron oxides and hydroxides. Like Fe, these elements are characterized by a slight downcore decrease of concentrations (Fig. 5). It is worth noting that the behavior of elements of the first group is retained in the black sediments (below 365–400 cm), but their fluctuation range is narrower relative to that in the overlying gray sediments. Thus, the hydrotroilite content, which is responsible for the black color, has a certain impact on the chemical composition of sediments. Elements of the second group (Th, U, Ba, Zr, Zn, Se, As; Eu, Tb, Yb, and Lu) were mainly absorbed by clay minerals. Precisely this type of sorbent distribution was reported for rare earth elements in (Gurvich *et al.*, 1980). Generally, these elements are character-

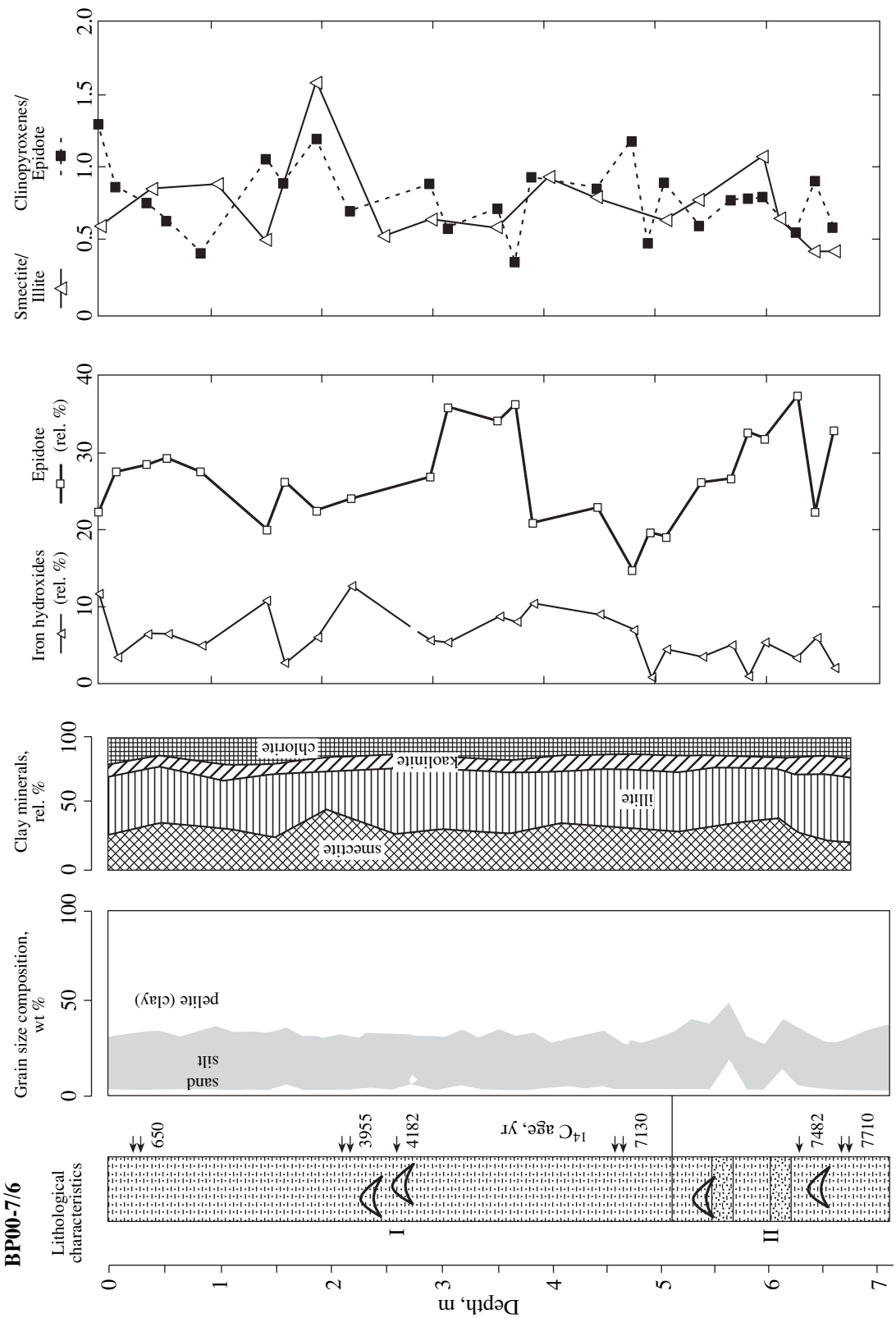

Fig. 4. Mineral composition of sediments in Core BP00-07/6 and distribution of some minerals in them. (I, II) Lithostratigraphic units. Normal and double arrows show the radiocarbon dates, respectively, for Core BP00-07/6 (see Table 1) and Core BP00-07/7 (Stein *et al.*, 2002). Legend as in Fig. 2.

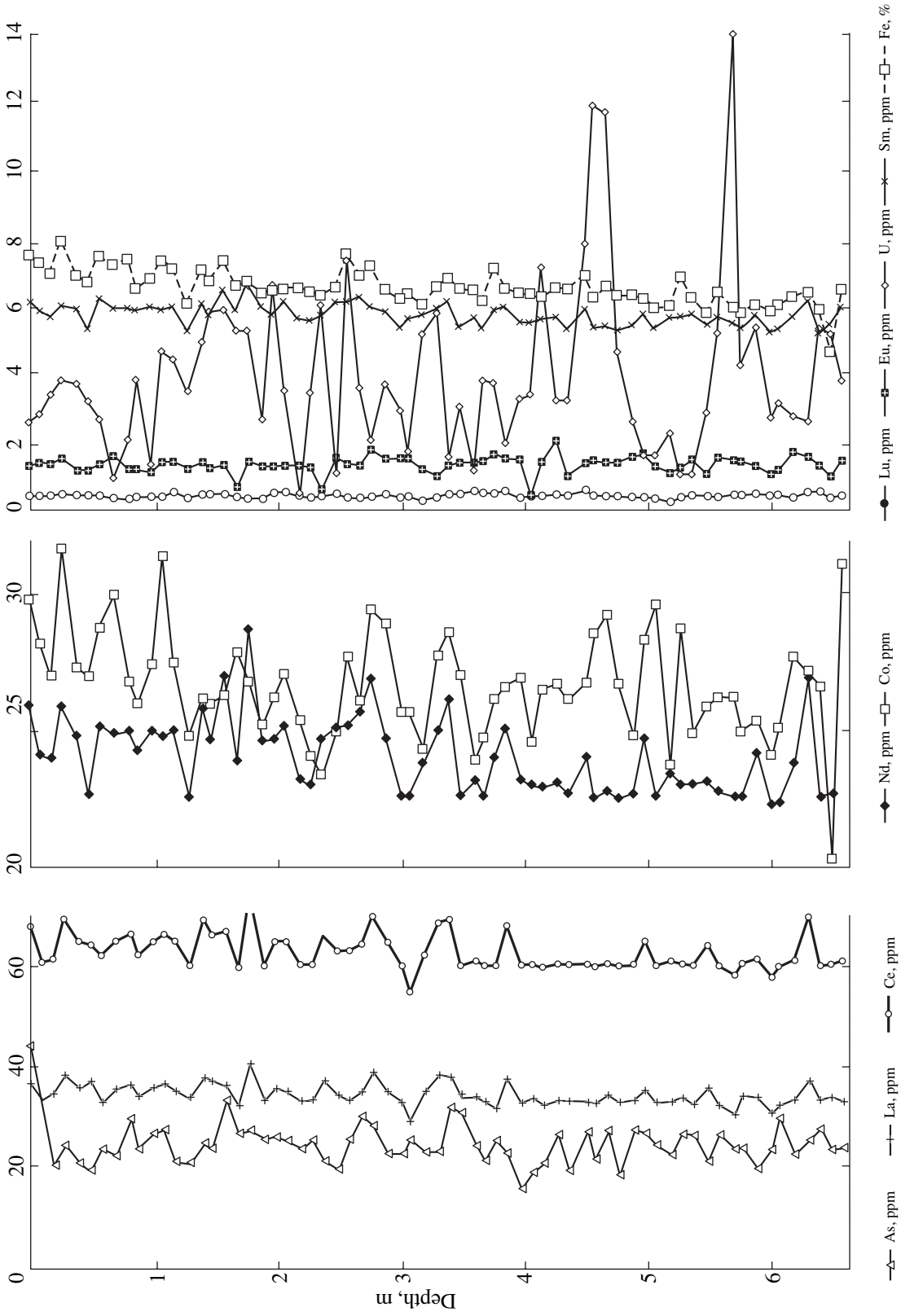

Fig. 5. Vertical distribution of some chemical elements and their ratios in Core BP00-07/6.

ized by a stable average value across the section (Fig. 5), except for As and U. The As content drastically increases in surface sediments, probably, owing to technogenic contamination (Siegel *et al.*, 2001a, 2001b). The U concentration is marked by rare maximums presumably related to the presence of organic matter in individual interlayers (Fig. 5).

Sedimentation and sedimentary mass accumulation rates. Calculations of sedimentation rate in Core BP00-23/7 are based on the following two assumptions. First, our observations revealed that gravity corers disintegrated the 0–15 interval of fine pelitic sediment. Therefore, the thickness of the uppermost interval, for which we calculated the sedimentation rate, was increased by 15 cm. Second, the study of magnetic susceptibility of some cores recovered at Station BP00-07 (Dittmers *et al.*, 2001) revealed that sediments in them are identical to each other in terms of their position in the section; i.e., neither the bottom depth nor the geological setting of the section at the station beneath the research vessel changed in the course of coring. Therefore, we assume that radiocarbon dates related to Core BP00-07/7 (Stein *et al.*, 2002) be used in our calculations (Fig. 4). They showed that the sedimentation rate was very high (789.5 cm/ka) at 8133–7905 yr BP00 (i.e., the time of Unit 2 formation), resulting in a high mass accumulation rate (525.0 g/cm^2/ka). In our opinion, such high values can be obtained only in the case of the existence of submarine slide in the specified geological setting. This assumption is additionally supported by the virtually similar ages of sediments at 510 cm (7905 yr BP00) and 645 cm (7875 yr BP00). After 7.9 ka BP00, the sedimentation and mass accumulation rates were in the range of 57.6–93.4 cm/ka and 31.6–47.6 g/cm^2/ka, respectively, until 268 yr BP00 when they increased to 171.6 cm/ka and 72.1 g/cm^2/ka, respectively.

Sedimentation history. The Ob–Yenisei shallow-water zone, which hosts Station BP00-07/7, is a late Pleistocene flooded alluvial plain. Its geological evolution in the late Pleistocene–Holocene was mainly governed by the global eustatic rise of the World Ocean level (Fairbanks, 1989) and the subordinate irregular supply from the Yenisei River runoff. The ocean level rise promoted the successive southward migration of the coastal zone and the consequent migration of the Yenisei marginal filter. One can assess the solid material runoff of the Yenisei River based on indicators of fluvial materials in the sediments, such as wood remains (Levitan, 2001) and high clinopyroxene/epidote and smectite/illite ratios (Levitan *et al.*, 1996).The heavy mineral composition shows that the river impact is best reflected in the clinopyroxene and iron hydroxide contents and, primarily, the clinopyroxene/epidote ratio (Fig. 6). Based on plant remains and the composition of sediments, the river runoff is most prominent in sediments with an age of 7.5–6.2 and 3.3–2.4 ka cal BP00. Correspondingly, the runoffs were minimal 6.2–3.3 and 2.4–1.4 ka BP00. The role of the Yenisei River runoff began to increase since ~1.4 ka BP00. At present, this influence is very significant and reflects the global warming in the 20th century.

Our data match the magnetic susceptibility (Stein *et al.*, 2003) and ostracode and mollusk (Taldenkova *et al.*, 2003) data on Core BP00-07/5. Our data also demonstrate a partial correlation with the oxygen and carbon isotope data on ostracode shells (Simstich *et al.*, 2003) and weak correlation with benthic foraminifer data on this core (Ivanova, 2003)

It should be noted that the assumption of the existence of submarine slide in the lower section of Core BP00-07/7 is supported not only by the radiocarbon dates, but also by the absence of bulk density variation within Unit 2 and its specific grain size composition. Interpretation of Unit 2 as a part of the marginal filter contradicts data on the distribution of indicators of the river runoff.

Thus, the studied southern Kara Sea sediments accumulated during the last 7.9 ka in the process of the Holocene transgression. The transport of pelitic particles from the surrounding seamounts by bottom currents and the Yenisei River runoff portion, which surmounted the marginal filter, served as the main sources of sedimentary material. As was shown above, the relationship between these sources repeatedly changed during the considered period. In general, the available data make it possible to emphasize that the BP00-07/7 area remained beyond the marginal filter in the considered period even during the most active delivery of the Yenisei material.

Core DM-4401 described in (Polyak *et al.*, 2002) is located in a channel, a tributary of the ancient Yenisei River, between cores Core BP00-07/6 and BP0023/7 (Fig. 1).

We calculated the sedimentation and mass accumulation rates for Core DM-4401. The results show that these parameters were equal to 26.7 cm/ka and 22.6 g/cm^2/ka, respectively, in the period of 0–3.27 ka BP00; 17.2 cm/ka and 17.6 g/cm^2/ka, respectively, in the period of 3.27–7.92 ka BP00; and 120.6 cm/ka and 106.1 g/cm^2/ka, respectively, in the period of 7.92–8.28 ka BP00. The latest sedimentation rate was probably retained until the 353-cm level that may be slightly older than 9.4 ka. The downcore portion up to the base (415 cm) is filled with coarser-grained sediments with very distinct signs of river influence (high clinopyroxene contents and clinopyroxene/epidote ratios, high concentrations of plant remains and fresh-water diatom frustules, and light oxygen isotopic composition of benthic foraminiferal tests). We assume higher sedimentation rates and marginal-filter setting for this portion.

Thus, we have recorded a strong influence of river runoff in Core DM-4401 area in the early Holocene (until 9.4 ka BP00?). The analysis of all indicators suggests that this influence diminished in the period up to 7.2 ka BP00 and then slightly increased up to the level of ~1.5 ka BP00. Data on the further period are contra-

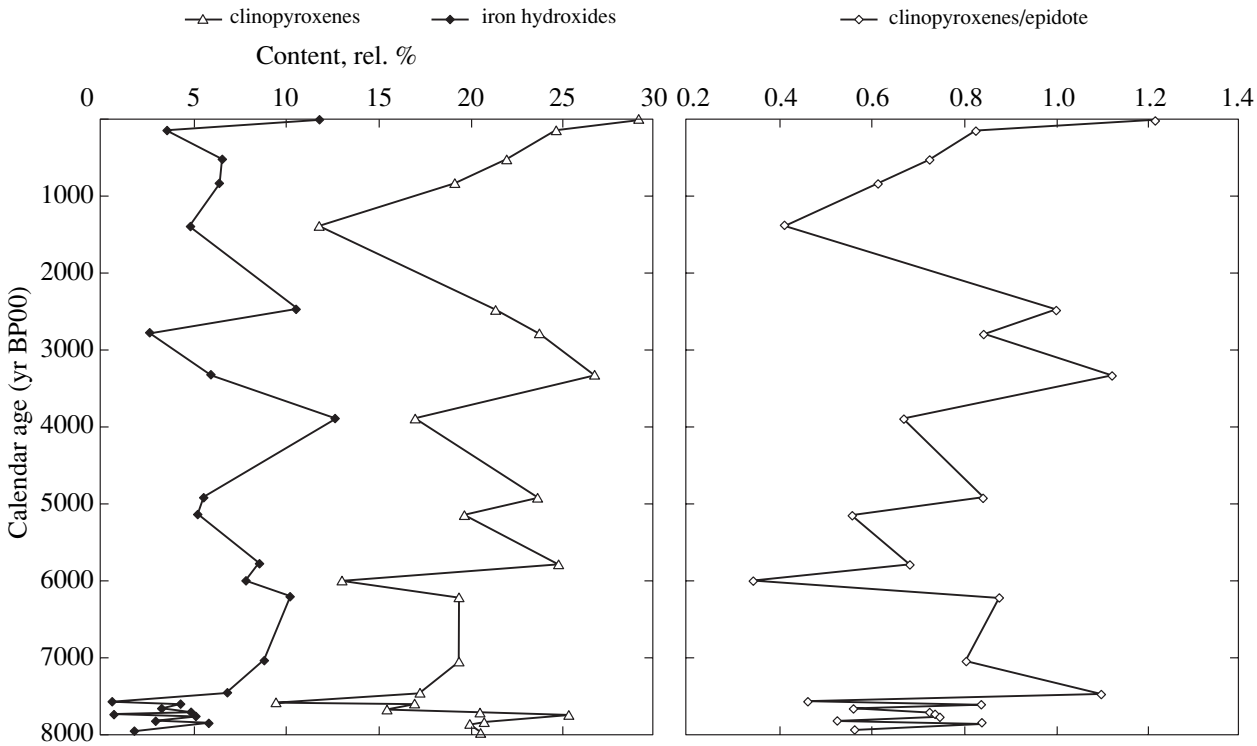

Fig. 6. Age distribution of some heavy minerals and their ratios in Core BP00-07/6.

dictory. Data on heavy minerals indicate an appreciable decrease of the Yenisei runoff contribution, while the diatom data suggest the contrary effect, i.e., increase of the Yenisei contribution. This may be caused by different mechanisms of the transport of heavy minerals, on the one hand, and the diatoms, on the other hand. In the first case, one can expect the preferential transport of heavy minerals in the nepheloid layer of the bottom water mass (Levitan *et al.*, 1996); in the second case, the preferential transport took place in the surface water. This assumption is supported by our data on the Ni/Al ratio in the sediments of Core DM-4401. This ratio serves as a facies indicator of the Yenisei River runoff (Schoster and Stein, 1999) and primarily reflects the composition of pelitic (clayey) fractions mainly transported in surface waters. Based on these assumptions, we found that the Ni/Al ration is more than 12.4×10^{-4} in the sediments younger than 3.27 ka and varies from 10.1 to 11.0×10^{-4} in older sediments (up to the core base).

History of Holocene Sedimentation along the Yenisei Transect in the Southern Kara Sea

The studied cores belong to two large facies zones of shelf sedimentation—the mixing zone of river and sea waters in the Gulf of Yenisei (Yenisei marginal filter) and the ancient river valley of a tributary of the ancient Yenisei River on the Ob–Yenisei shallow-water zone. We have revealed that each of these facies zones is characterized by the specific Holocene sedimentation history (Levitan *et al.*, 1996). We have reconstructed the following historical–geological succession of submarine deltaic sediments by the mixing zone sediments for the marginal filter: proximal sediments, depocenter sediments accumulated at avalanche rates, and distal sediments with the contribution of coastal abrasion products. The major portion of the geological body of the marginal filter in the study area formed within a very short time span (9.6–9.2 ka BP00).

Based on various facies indicators, we have deciphered the following periods of strong influence of river runoff in the northern Core BP00-07/6 area, ka BP00: 7.5–6.2, 3.3–2.4, and 1.4–0. The basal core section probably represents a part of the submarine slide.

In general, the Holocene sedimentation history of the southern Kara Sea is related to synchronous processes of the global eustatic rise of the World Ocean level (Fairbridge, 1989; Stein *et al.*, 2002), subsidence compensated by sedimentation in the Yenisei marginal filter (Gurevich, 1995), and fluctuating Yenisei River runoffs. Concepts of the variable basin depth (Stein *et al.*, 2002) suggest that the Atlantic water did not penetrate the study area.

One should first judge about the scale of the Yenisei River runoff based on the mass accumulation rate of fluvial material. This value is maximal in the depocenter. The comparison of all available data on the Yenisei transect (Fig. 1) reported in (Polyak *et al.*, 2002; Stein *et al.*, 2002) with data in the present com-

munication shows a north-to-south rejuvenation trend of the marginal-filter (more precisely, its depocenter) boundary with the overlying marine shelf sediments: 11.0 ka in Core BP00-36/4, 9.8 ka in Core BP00-26/4, 9.4 (?) ka in DM-4401, 9.2 ka in Core BP00-23/7, and 8.8 ka in Core BP00-04/7 (sediments of cores BP00-07/5, BP00-07/6, and BP00-07/7 did not reach this boundary). This is caused by the southward Flandrian transgression owing to the global eustatic sealevel rise. The transgression rate was approximately 146 km/ka (probably, up to 100*n* km/ka) in the early Holocene in the southern Kara Sea and decreased to 22 km/ka in the later period (within the present-day marginal filter zone). This difference in transgression rate could be linked to the deepening of the northern areas of the Barents and Kara seas during the deglaciation and early Holocene as a result of glacial isostasy (Lubinskii *et al.*, 2001). The southern Kara Sea did not undergo such deepening. At the same time, the distinction can also be explained by a higher rise rate of the World Ocean level 11.0–9.5 ka BP00 relative to 9.5–8.0 ka BP00 (Fairbanks, 1989). We believe that the latter reason is more probable, because this process is global. However, one cannot rule out the simultaneous impact of both factors.

The subsequent fluctuations of the Yenisei River runoff were commonly characterized by one or more order of magnitude lesser values relative to the early Holocene ones. Depending on the nature and mechanism of transport, various indicators of the fluvial material indicate different periods of the intensification or attenuation of the Yenisei River runoff in each of the studied cores.

ACKNOWLEDGMENTS

We are grateful to L.V. Polyak for assistance in the analysis of four mollusk samples by the AMS C-14 method in the Arizona University accelerator facility. We thank R. Stein (AWI, Bremerhaven, Germany) for placing at our disposal radiocarbon dates on Core BP00-07/7 before their publication. This work benefited from discussions of several historical–geological aspects of the interpretation of Core BP00-07/6 data with J. Simstich (Cambridge University, Great Britain). The discussion of geochemical aspects with A.A. Migdisov was also very fruitful.

This work was supported by the Russian Foundation for Basic Research (project no. 02-05-64017) and the Federal Program "World Ocean" (project no. 43.634.11).

REFERENCES

Aagaard, K. and Carmack, E.C., The Role of Sea Ice and Other Fresh Water in the Arctic Circulation, *J. Geophys. Res.*, 1989, vol. 94 (C10), pp. 14485–14498.

Artem'ev, V.E., *Geokhimiya organicheskogo veshchestva v sisteme reka-more* (Organic Mater Geochemistry in the River–Sea System), Moscow: Nauka, 1993.

Balashov, Yu.A., *Geokhimiya redkozemel'nykh elementov* (Geochemistry of Rare Earth Elements), Moscow: Nauka, 1976.

Belov, N.A. and Lapina, N.N., *Donnye osadki Severnogo Ledovitogo okeana* (Bottom Sediments in the Arctic Ocean), Leningrad: Gidrometeoizdat, 1961.

Dai, M.-H. and Martin, J.-M., First Data on Trace Metal Level and Behavior in Two Major Arctic River-Estuarine Systems (Ob and Yenisei) and in the Adjacent Kara Sea, Russia, *Earth Planet. Sci. Lett.*, 1995, vol. 131, pp. 127–141.

Dittmers, K., Stein, R., and Steinke, T., Core Logging: Magnetic Susceptibility, *Ber. Bunsen-Ges. Phys. Chem. Polarforsch.*, 2001, no. 393, pp. 89–91.

Fairbanks, R.G., A 17.000-Year Glacio-Eustatic Sea Level Record: Influence of Glacial Melting Rates on the Younger Dryas Event and Deep Ocean Circulation, *Nature* (London), 1989, vol. 342, pp. 637–642.

Frolov, V.T., *Litologiya* (Lithology), Moscow: Mosk. Gos. Univ., vol. 1, 1995.

Geologicheskoe stroenie SSSR i zakonomernosti razmeshcheniya poleznykh iskopaemykh (Geological Structure of the USSR and Location of Mineral Resources), vol. 9: Seas of the Soviet Arctic, Leningrad: Nedra, 1984.

Gurevich, V.I., *Recent Sedimentogenesis and Environment on the Arctic Shelf of Western Eurasia*, Oslo, Norsk Polarinst., 1995.

Gurvich, E.G., Isaeva, A.B., Demina, L.V., *et al.*, Chemical Composition of Bottom Sediments in the Kara Sea and Ob–Yenisei Estuarine System, *Okeanologiya*, 1994, no. 5, pp. 766–775.

Gurvich, E.G., Lukashin, V.N., Lisitsyn, A.P., and Kurinov, A.D., Rare Earth Elements and Yttrium, *Geokhimiya elementov-gidrolizatov* (Geochemistry of Hydrolyzate Elements), Moscow: Nauka, 1980, pp. 71–116.

Hald, M., Kolstad, V., Polyak, L., *et al.*, Late-Glacial and Holocene Paleoceanography and Sedimentary Environments in the St. Anna Trough, Eurasian, Arctic Ocean, *Palaeogeogr. Palaeoclimatol. Palaeoecol.*, 1999, vol. 146, pp. 229–249.

Ivanova, E., Benthic Foraminifera in Sediments from the Southern Kara Sea: Preliminary Results, *Ber. Bunsen-Ges. Phys. Chem. Polarforsch.*, 2001, no. 393, pp. 141–150.

Ivanova, E.V., Benthic Foraminiferal Assemblages of the Kara Sea: Response to Salinity Variation during the Holocene, *Program and Abstracts: 4th Int. Workshop SIRRO*, Moscow: Geol. Khim. Inst., 2003.

Khusid, T.A. and Korsun, S.A., Modern Benthic Foraminiferal Assemblages in the Kara Sea, *Ber. Polarforsch.*, 1996, no. 212, pp. 308–314.

Kodina, L.A., Tokarev, V.G., Sukhoruk, V.I., *et al.*, Preliminary Results of Geochemical Investigations of Sediment Cores along the Yenisei Profile (Acoustic Units I-II), *Ber. Polarforsch.*, 2001, no. 393, pp. 179–184.

Kolesov, G.M., The Identification of Minor elements: Neutron Activation Analysis in Geochemistry and Cosmochemistry, *Zh. Anal. Khim.*, 1994, vol. 49, no. 1, pp. 55–66.

Kosheleva, V.A. and Yashin, D.S., *Donnye osadki arkticheskikh morei* (Bottom Sediments in the Arctic Seas), St. Petersburg: Vses. Nauchn.-Issled. Inst. Okeangeologiya, 1999.

Levitan, M., Facies Variability of Surface Sediments along the Yenisei Transect Based on Grain-Size Composition, Heavy and Light Mineral Data, *Ber. Polarforsch.*, 2001, no. 393, pp. 92–106.

Levitan, M.A., Arnold, M., Burtman, M.V., *et al.*, On the History of Holocene Sedimentation in the Eastern Kara Sea, *Okeanologiya*, no. 4, pp. 614–620 [Oceanology, 2000, no. 4, pp. 577–582].

Levitan, M.A., Bourtman, M.V., Gorbunova, Z.N., and Gurvich, E.G., Quartz and Feldspars in the Surface Layer of Kara Sea Sediments, *Litol. Polezn. Iskop.*, 1998, vol. 33, no. 2, pp. 115–125 [Lithol. Miner. Resour., 1998, vol. 33, no. 2, pp. 99–108].

Levitan, M.A., Dekov, V.M., Gorbunova, Z.N., *et al.*, The Kara Sea: A Reflection of Modern Environment in Grain Size, Mineralogy, and Chemical Composition of the Surface Layer of Bottom Sediments, *Ber. Polarforsch.*, 1996, no. 212, pp. 58–80.

Levitan, M.A., Khusid, T.A., Kuptsov, V.M., *et al.*, Upper Quaternary Sedimentary Sequence Types in the Kara Sea, *Okeanologiya*, 1994, no. 5, pp. 776–788.

Levitan, M.A., Kolesov, G., and Chudetsky, M., Chemical Characteristics of Main Lithofacies Based on Instrumental Neutron-Activation Analysis Data, *Ber. Polarforsch.*, 2002, no. 419, pp. 101–111.

Lightfoot, P.C., Naldrett, A.J., Gorbachev, N.S., *et al.*, Geochemistry of the Siberian Trap of the Norilsk Area, USSR, with Implication for the Relative Contributions of Crust and Mantle to Flood Basalt Magmatism, *Contrib. Mineral. Petrol.*, 1990, vol. 104, pp. 631–644.

Lubinski, D.J., Polyak, L., and Forman, S.L., Deciphering the Latest Pleistocene and Holocene Inflows of Freshwater and Atlantic Water to the Deep Northern Barents and Kara Seas: Foraminifera and Stable Isotopes, *Quatern. Sci. Rev.*, 2001, vol. 20, pp. 1851–1879.

MacDonald, G.M., Velichko, A.A., Kremenetski, C.V., *et al.*, Holocene Treeline History and Climate Change across Northern Eurasia, *Quaternary Res.*, 2000, vol. 53, pp. 302–311.

Petelin, V.P., *Granulometricheskii analiz morskikh donnykh osadkov* (Grain Size Distribution Analysis of Marine Bottom Sediments), Moscow: Nauka, 1967.

Polyak, L., Forman, S.L., Herlihy, F.A., *et al.*, Late Weichselian Deglacial History of the Svyataya (Saint) Anna Trough, Northern Kara Sea, Arctic Russia, *Mar. Geol.*, 1997, vol. 143, pp. 169–188.

Polyak, L., Levitan, M., Gataullin, V., *et al.*, The Impact of Glaciation, River-Discharge and Sea-Level Change on Late Quaternary Environments in the Southwestern Kara Sea, *Int. J. Earth Sci.*, 2000, vol. 89, pp. 550–562.

Polyak, L., Levitan, M., Khusid, T., *et al.*, Variations in the Influence of Riverine Discharge on the Kara Sea during the Last Deglaciation and the Holocene, *Global Planet. Change*, 2002, vol. 32, pp. 291–309.

Polyakova, Ye. and Stein, R., Holocene Variations in the Eurasian, Arctic Shelf Surface Water Salinity and Sea Ice Regime: Evidences from Diatom Assemblages of the Siberian Arctic Shelf, Kara Sea, *Program and Abstracts: EMMM' 2002*, Vienna, 2002, pp. 164–165.

Schoster, F. and Stein, R., Major and Minor Elements in Surface Sediments of Ob and Yenisei Estuaries and the Adjacent Kara Sea, *Ber. Polarforsch.*, 1999, no. 300, pp. 196–207.

Sedykh, E.M., Starshinova, N.P., Bannykh, L.N., *et al.*, Identification of Heavy Metals and Their Forms in Waters and Bottom Sediments of Water Reservoirs Based on Methods of the Atomic Emission Spectrometry with Inductive-Coupled Plasma and Electrothermal Atomic Absorption Spectrometry, *Zh. Anal. Khim.*, 2000, vol. 55, no. 4, pp. 385–391.

Siegel, F.R., Galasso, J.J., and Kravitz, J.H., Geochemistry of Thirteen Voronin Trough Cores, Kara Sea, European Arctic: Hg and As Contaminants at a 1965 Timeline, *Appl. Geochem.*, 2001a, vol. 16, pp. 19–34.

Siegel, F.R., Kravitz, J.H., and Galasso, J.J., Arsenic and Mercury Contamination in 31 Cores Taken in 1965, St. Anna Trough, Kara Sea, Arctic Ocean, *Environ. Geol.*, 2001b, vol. 40, pp. 528–542.

Simstich, J., Stanovoy, V., Bauch, D., Erlenkeuser, H., and Spielhagen, R.F., Holocene Variability of Bottom Water Hydrography on the Kara Sea Shelf Depicted in Multiple Single-Valve Analysis of Stable Isotopes in Ostracods, *Program and Abstracts: 4th Int. Workshop SIRRO*, Moscow, Geol. Khem. Inst., 2003.

Stein, R., Lithostratigraphy of Gravity Cores and Correlation with Sediment Echograph Profiles ("Akademik Boris Petrov" Kara Sea Expeditions, 1999, and 2000), *Ber. Polarforsch.*, 2001, no. 393, pp. 120–140.

Stein, R. and Levitan, M., Lithological Core Description, *Ber. Polarforsch.*, 2001, no. 393, pp. 247–283.

Stein, R., Boucsein, B., Hefter, J., *et al.*, Marine Geology, *Ber. Polarforsch.*, 2000, no. 360, pp. 49–69.

Stein, R., Dittmers, K., Fahl, K., *et al.*, Terrigenous Sediment Supply in the Holocene Kara Sea: Sources, Burial, Variability and Paleoenvironment, *Program and Abstracts: 4th Int. Workshop SIRRO*, Moscow: Geol. Khim. Inst., 2003, pp. 30–32.

Stein, R., Niessen, F., Dittmers, K., *et al.*, Siberian River Run-Off and Late Quaternary Glaciation in the Southern Kara Sea, Arctic Ocean: Preliminary Results, *Polar Res.*, 2002, vol. 21, pp. 315–322.

Stuiver, M., Reimer, P.J., Bard, E., *et al.*, INTCAL 98 Radiocarbon Age Calibration, 24,000-0 Cal BP00, *Radiocarbon*, 1998, vol. 40, pp. 1041–1083.

Taldenkova, E., Stepanova, A., and Simstich, J., Downcore Variations in Species Composition of Ostracods and Mollusks in Core BP00-07/5 and Some Paleoenvironmental Implementations, *Program and Abstracts: 4th Int. Workshop SIRRO*, Moscow: Geol. Khim. Inst., 2003.